Nano Energy 52 (2018) 517–523

Contents lists available at ScienceDirect

Nano Energy

journal homepage: www.elsevier.com/locate/nanoen

Full paper

Theory of contact electrification: Optical transitions in two-level systems

Morten Willatzen[a,b,*], Zhong Lin Wang[a,b,c]

[a] CAS Center for Excellence in Nanoscience, Beijing Key Laboratory of Micro-nano Energy and Sensor, Beijing Institute of Nanoenergy and Nanosystems, Chinese Academy of Sciences, Beijing 100083, PR China

[b] School of Nanoscience and Technology, University of Chinese Academy of Sciences, Beijing 100049, PR China

[c] School of Materials Science and Engineering, Georgia Institute of Technology, Atlanta, GA 30332-0245, USA

ARTICLE INFO

Keywords:
Quantum mechanics
Contact electrification
Triboelectric nanogenerators

ABSTRACT

The increasing need to power networks of trillions of sensors and devices for the Internet of Things requires effective generators to harvest low-frequency ambient mechanical vibrations. This type of energy is different from conventional power because it is mobile, widely distributed and involves the coupling of a huge amount of units. Triboelectric nanogenerators are ideal candidates for this purpose and can provide power densities up to 500 W/m^2 or 15 MW/m^3. While the phenomenon of triboelectricity has been known and explored since ancient history, a detailed microscopic understanding is still under debate. Recent experimental study has proposed a general model in which triboelectrification may be a result of electron transfer between two atoms owing to the lowered barrier due to overlapped electron clouds (Xu et al. [13]). Here, we provide, in the context of the proposed triboelectric model, a first quantum-mechanical calculation of electron transfer and light coupling between two dissimilar atoms interacting at a distance based on the one-electron Schrödinger model and the Fermi Golden Rule. Static and dynamic studies of contact electrification and photon emission between two groups of atoms are also analyzed. Despite the model's simplicity in addressing coupled atoms it may set the frame for a better understanding and exploitation of charge transfer in nanotriboelectric systems consisting of many atoms or solids.

1. Introduction

An increasing challenge, central to the Internet of Things, is to provide, ubiquitously, easy access to power a huge number of sensors without the use of batteries. Since triboelectric nanogenerators (TENGs) are the best candidates to meet this challenge and harvest low-frequency ambient vibrations, major efforts are necessary to understand better the fundamental and microscopic nature of contact electrification (CE) and to use this knowledge in improving TENG performance in different applications. Traditionally, the most important approach for harvesting ambient mechanical energy has been electromagnetic generators (EMGs). EMGs are efficient at high frequencies (substantially above 10 Hz) [16] but a vast amount of ambient mechanical energy, such as as ocean wave energy and human body motion, is available at frequencies below 5 Hz [17,18]. The most powerful approach to harvest energy under low-frequency motion (>5 Hz) is to use TENG [14–16,19–23] that operate in four basic modes: Vertical contact-separation mode [24], lateral sliding mode [25], single-electron mode [26], and free-standing triboelectric-layer mode [27].

Triboelectrification or contact electrification in scientific terms is a phenomenon known for more than 2600 years yet a fundamental understanding of its origin is still under debate [1,2]. Both electron and ion transfer mechanisms play a role in CE but the strengths of the two contributions depend intricately on the contact materials. In metal-metal (MM) and metal-semiconductor (MS) systems electron transfer is well described by the work function of contact potential difference between the two materials [3,4]. For the metal-insulator (MI) system, both electron [5–7] and ion transfer [8–12] mechanisms were long believed to play a role. Electron transfer in MI systems exists by virtue of surface state coupling. A recent paper by the group of Zhong Lin Wang [13] has revealed that also for MI systems, electron transfer dominates CE. They discovered the temperature dependence of CE, and the phenomenon vanishes once the temperature reached approximately 280 °C owing to electron thermionic emission. As a result, a model for electron transfer was proposed with considering electron transfer due to the lowered barrier between the two atoms as they are forced together. Here, a quantum mechanical calculation is proposed to quantitatively illustrate the electron-cloud-potential-well model for explaining charge transfer and release between two materials that may not have a well specified energy band structure.

* Corresponding author.
E-mail addresses: morwi@fotonik.dtu.dk, mortenwillatzen@binn.cas.cn (M. Willatzen).

https://doi.org/10.1016/j.nanoen.2018.08.015
Received 11 July 2018; Received in revised form 7 August 2018; Accepted 8 August 2018
Available online 11 August 2018
2211-2855/

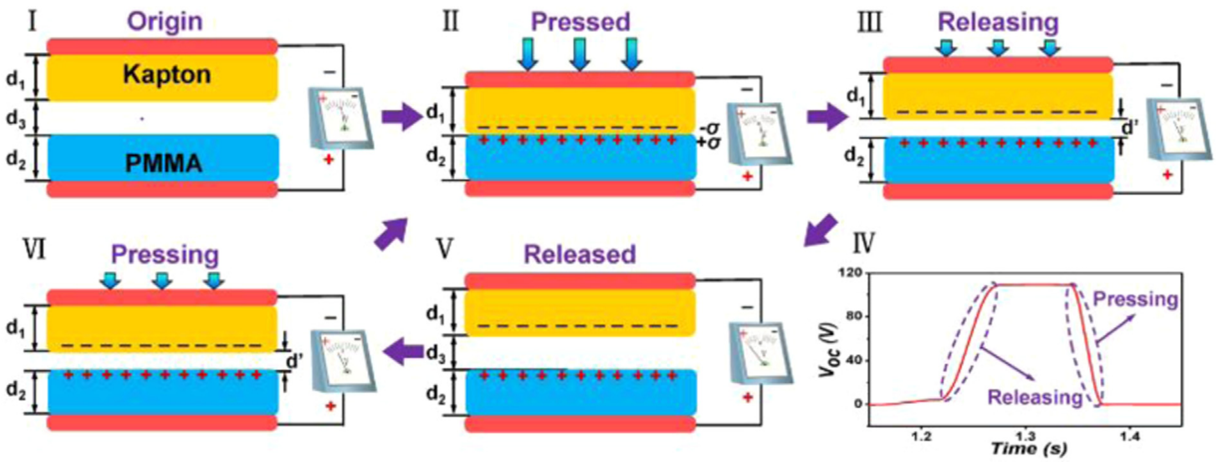

Fig. 1. Triboelectric effect: electron transfer between two dissimilar dielectric materials in contact. From Zhu et al. [24].

The model estimates the probability electron transfer and predicts a light emission of distinct but coupled atomic systems as a function of the distance between the atoms. As such, the model sheds new light on the perspectives for efficient energy harvesting and photonic control based on TENGs.

2. Experimental background

The principle behind the triboelectric nanogenerator invented in 2012 is to utilize the potential created by surface triboelectric charges for driving the flow of electrons between two electrodes. Fig. 1 shows a simple mode of TENG operation, in which two dielectric films made of dissimilar materials are coated with metal electrodes at their top and bottom surfaces, respectively. Upon physical contact, triboelectric charges are created at the dielectric surfaces. Once the two films are separated by an external force, electrons in the electrodes will be driven to flow in order to balance the electrostatic potential built by the triboelectric charges, leading to a new technology for converting mechanical energy into electricity. The core of TENG is contact electrification. In order to explain the electron transfer between two general materials, Xu et al. [13] suggested a two atom model (Fig. 2), one of which belongs to material A and the other belongs to material B. If the two atoms are separated by a relatively large distance, electrons are tightly bounded to the nuclei of either atoms A or B, and there is no charge transfer. Once the two atoms are brought close together, the wave functions or electron clouds of the two atoms start to overlap. As a result, the potential barrier between the two is reduced, resulting in a possibility of an electron to transfer from atom A to atom B, which is suggested as a simple model of contact-electrification. Our task now is to present a theoretical model to calculate quantitatively the electron transfer from atom A to atom B as a function of their interatomic distance. In this simple model, photons can be emitted due to coupling of two electron levels associated with dissimilar atoms, a process which remains to be verified experimentally.

3. Optical absorption in a semiconductor

In this section [28], we discuss the absorption coefficient of photons by a two-level system in a medium of refractive index $n(\omega)$. Firstly, we introduce the one-electron description of electrons coupled to an electromagnetic vector potential. This coupling leads to level transitions and can be treated in a perturbative way by use of the Fermi Golden Rule for calculation of the photon emission/absorption rate.

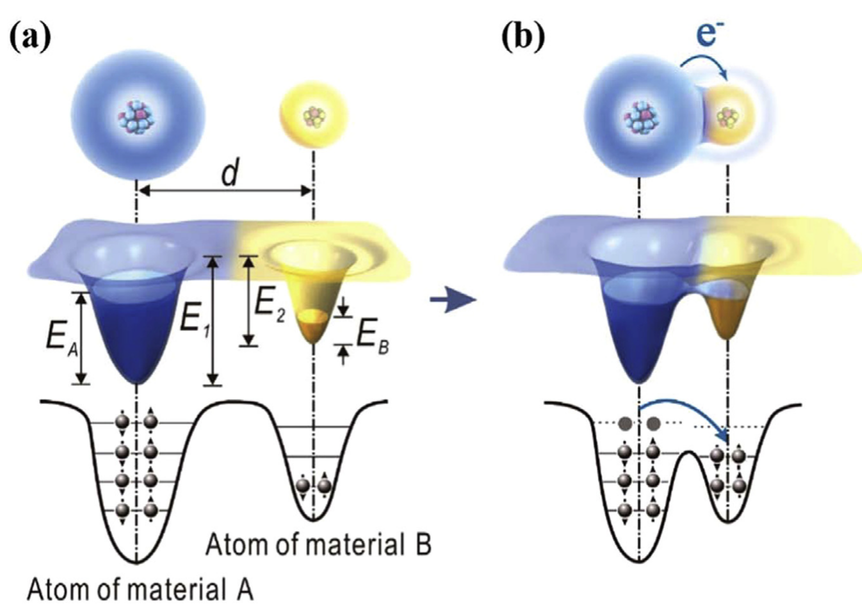

Fig. 2. Electron transfer between two atoms A and B in contact. From Xu et al. [13].

4. A nonrelativistic description of the electron-photon interaction

A simple, and to a large extent adequate, description of electrons in a potential $V(\mathbf{r})$ is given by the one-particle Schrödinger equation

$$H\psi(\mathbf{r}) = E\psi(\mathbf{r}), \tag{1}$$

$$H = \frac{\mathbf{p}^2}{2m_0} + V(\mathbf{r}) = -\frac{\hbar^2\nabla^2}{2m_0} + V(\mathbf{r}), \tag{2}$$

where $\psi(\mathbf{r})$ is the electron wavefunction, E is the energy eigenvalue, $\mathbf{p}$ is the momentum operator, and m_0 is the free-electron mass. We know from classical mechanics that the presence of an electromagnetic field modifies the Hamiltonian in Eq. (1) according to the replacement

$$\mathbf{p} \to \mathbf{p} - e\mathbf{A}(\mathbf{r}, t), \tag{3}$$

where $\mathbf{A}(\mathbf{r}, t)$ is the electromagnetic vector potential satisfying

$$\mathbf{E}\left(\mathbf{r}, t\right) = -\frac{\partial \mathbf{A}(\mathbf{r}, t)}{\partial t}. \tag{4}$$

In Eq. (4), $\mathbf{E}(\mathbf{r}, t)$ is the electric field. Inserting Eq. (3) in Eq. (2) leads to the following expression for the interaction Hamiltonian H_{int}

$$H = H_0 + H_{int},$$

$$H_{int} - \frac{e}{m_0}\mathbf{A}\left(\mathbf{r}, t\right)\cdot\mathbf{p}, \tag{5}$$

where H_0 is the unperturbed Hamiltonian ($H_0 \equiv H$ in Eq. (1)). Here, it has been used that terms to second order in $\mathbf{A}$ commutes with $\mathbf{p}$ due to the transversality condition $\nabla\cdot\mathbf{A}(\mathbf{r}, t) = 0$.

The electron-photon interaction given by the Hamiltonian H_{int} in Eq. (5) induces optical transitions between the two levels because momentum matrix elements in general are non-vanishing. This is the case even if the two levels have the same symmetry, e.g., S atomic states, if they are centered at different atoms. We can obtain information about optical absorption, spontaneous emission etc. in a two-level system (and later a crystal) by use of time-dependent perturbation theory.

5. Absorption and spontaneous emission in a two-level system

For a simple two-energy level system, the emission rate between an initial state of energy E_i and a final state of energy E_f is given by the *Golden Rule*

$$W = \frac{2\pi}{\hbar}|\langle f|H_{int}^e|i\rangle|^2\rho(E)\delta(E - E_i + E_f), \tag{6}$$

where H_{int}^e is the time-independent part of the interaction Hamiltonian H_{int} responsible for emission of photons according to

$$H_{int} = H_{int}^e \exp\left(i\frac{E}{\hbar}t\right) + H_{int}^a \exp\left(-i\frac{E}{\hbar}t\right), \tag{7}$$

where superscripts e and a refer to emission and absorption, respectively.

For a plane wave with the angular frequency ω, the electric field is written as

$$\mathscr{E} = \boldsymbol{\varepsilon}\left(\frac{\mathscr{E}_0}{2}\exp(i\omega t) + c.\ c\right), \tag{8}$$

where $\boldsymbol{\varepsilon}$ is the unit polarization vector. An expression for the magnitude of the coefficient $\mathscr{E}_0$ associated with one photon can be found by evaluating the energy flux S using Maxwell's equations:

$$S = \frac{1}{2}|\mathscr{E}_0|^2 n\epsilon_0 c. \tag{9}$$

In Eq. (9), n is the refractive index of the medium. The energy flux is also given by the product of the photon energy denisty $\hbar\omega/V$ and the group velocity c/n_g so that

$$|\mathscr{E}_0| = \sqrt{\frac{2\hbar\omega}{nn_g\epsilon_0 V}}, \tag{10}$$

where V is the volume of the enclosure confining the electromagnetic field. The interaction Hamiltonian can now be written as

$$H_{int} = -\frac{e}{m_0}i\sqrt{\frac{\hbar}{2nn_g\epsilon_0\omega V}}\left[\exp(i(\delta + \omega t)) - \exp(-i(\delta + \omega t))\right]\boldsymbol{\varepsilon}\cdot\mathbf{p}, \tag{11}$$

where δ is defined from $\epsilon_0 = |\epsilon|\exp(i\delta)$ and Eqs. (5), (8), and (10) are used. The emission rate defined in Eq. (6) is given by

$$W = \frac{e^2h}{2m_0^2 nn_g\epsilon_0 EV}|\langle f|\boldsymbol{\varepsilon}\cdot\mathbf{p}|i\rangle|^2\rho(E)\delta(E - E_i + E_f), \tag{12}$$

using Eq. (11). In the case of stimulated emission or absorption for a two-level system $\rho(E) = 1$. In a similar way, we can obtain the absorption coefficient from the (stimulated) absorption rate. The absorption coefficient $\alpha(E)$ for photons of energy $E = \hbar\omega$ becomes

$$\alpha = \frac{e^2h}{2m_0^2 nc\epsilon_0 EV}|\langle f|\boldsymbol{\varepsilon}\cdot\mathbf{p}|i\rangle|^2\delta(E + E_i - E_f). \tag{13}$$

Here, $\alpha(E)$ is the number of photons absorbed per unit distance $\alpha(E) = \frac{n_g W}{c}$. Note that the absorption coefficient is proportional to $1/V$, because we consider absorption of a photon within a box of volume V by a single two-level system.

For spontaneous emission of $\boldsymbol{\varepsilon}$-polarized photons, on the other hand, the density of final states in a solid angle element $d\Omega$, $\rho_{d\Omega}(E)$ equals the number of photon states of energy E per unit volume per unit energy with wavevector pointing into $d\Omega$

$$\rho_{d\Omega}(E) = \frac{k^2 dk d\Omega}{(2\pi)^3 dE}. \tag{14}$$

Since $E = \hbar\omega$ and $k = n\omega/c$ we may write for the spontaneous emission rate into $d\Omega$ per unit volume at the photon energy E for $\boldsymbol{\varepsilon}$-polarized photons, $r_{sp,d\Omega}(E)$

$$r_{sp,d\Omega}(E) = \frac{ne^2 E d\Omega}{2m_0^2 c^3\epsilon_0 h^2\ V}|\langle f|\boldsymbol{\varepsilon}\cdot\mathbf{p}|i\rangle|^2\delta(E - E_i + E_f), \tag{15}$$

where

$$\frac{dk}{dE} = \frac{d\left(n\frac{\omega}{c}\right)}{d(\hbar\omega)} = \frac{1}{\hbar c}\frac{d(n\omega)}{d\omega} = \frac{1}{\hbar c}\left(n + \omega\frac{dn}{d\omega}\right) = \frac{n_g}{\hbar c}, \tag{16}$$

was used. So far, we have been concerned with a radiative transition in which a photon with definite propagation direction $\mathbf{k}$ and polarization $\boldsymbol{\varepsilon}$ is emitted. To get the total spontaneous emission rate per volume at the photon energy E, r_{sp}, we must sum over the two independent polarization directions for a given $\mathbf{k}$ and integrate over all possible propagation orientations. From Fig. 3 it is evident that

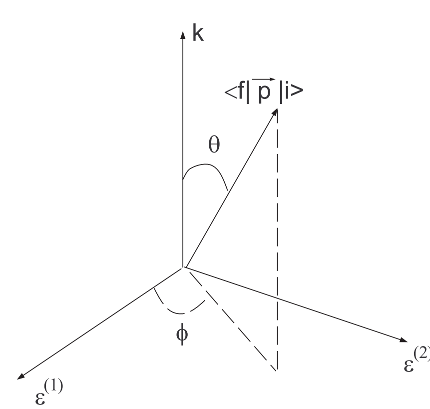

Fig. 3. Orientation of $\langle f|\mathbf{p}|i\rangle$.

$$|\langle f|\varepsilon^{(1)}\cdot\mathbf{p}|i\rangle| = |\langle f|\mathbf{p}|i\rangle|\sin\theta\cos\phi$$
$$|\langle f|\varepsilon^{(2)}\cdot\mathbf{p}|i\rangle| = |\langle f|\mathbf{p}|i\rangle|\sin\theta\sin\phi. \tag{17}$$

The sum over the two polarization states gives $\sin^2\theta$. Performing the integration over all possible angles, with $\langle f|\mathbf{p}|i\rangle$ fixed in space, gives $8\pi/3$, and we obtain

$$r_{sp} = \int r_{sp,d\Omega}(E)d\Omega = \frac{4\pi e^2 nE}{3m_0^2c^3\epsilon_0 h^2 V}|\langle f|\mathbf{p}|i\rangle|^2\delta(E - E_i + E_f). \tag{18}$$

In passing, we note that the spontaneous emission rate can be rewritten in terms of the dipole moment

$$\langle f|e\mathbf{r}|i\rangle, \tag{19}$$

by use of the commutator relation

$$\mathbf{p} = \frac{im_0}{\hbar}[H_0, \mathbf{r}]. \tag{20}$$

Using this result and multiplying the spontaneous emission rate in Eq. (18) by V we obtain for the total spontaneous emission rate at ω after integrating over energy E

$$R_{sp}(\omega) = \frac{\omega^3}{3\pi c^3\epsilon_0\hbar}|\langle f|e\mathbf{r}|i\rangle|^2, \tag{21}$$

which agrees with the result in Ref. [29].

6. Einstein *A* and *B* coefficients and rate equations

Let us first consider a system of N two-level atoms of the same material. We have, at any time, N_b (N_a) atoms for which the upper state $|2\rangle$ (lower state $|1\rangle$) is occupied and $N = N_a + N_b$. All N atoms are considered non-interacting and transitions can only take place between levels 1 and 2 of the same atom. The rate of spontaneous emission was found above, R_{sp}, which we will call A_{ba} to follow a traditional choice in the literature. Taking all processes into account, we find

$$\frac{dN_b}{dt} = -N_bA_{ba} - N_bB_{ba}\rho(\omega) + N_aB_{ab}\rho(\omega), \tag{22}$$

$$\frac{dN_a}{dt} = N_bA_{ba} + N_bB_{ba}\rho(\omega) - N_aB_{ab}\rho(\omega), \tag{23}$$

where the coefficient B_{ba} (B_{ab}) determines the rate of stimulated emission (absorption) of photons and $\rho(\omega)$ is the energy density in the field evaluated at $\omega = \frac{E_b - E_a}{\hbar}$. If in thermal equilibrium

$$\frac{dN_b}{dt} = \frac{dN_a}{dt} = 0, \tag{24}$$

and solving for ρ gives

$$\rho(\omega) = \frac{A_{ba}}{\frac{N_a}{N_b}B_{ab} - B_{ba}}. \tag{25}$$

Assuming Boltzmann statistics, the occupation number of a state m is proportional to $e^{-\frac{E_m}{k_BT}}$, where E_m, k_B, and T are the energy of level m, Boltzmann's constant, and the absolute temperature, respectively. Hence

$$\frac{N_a}{N_b} = e^{\frac{\hbar\omega}{k_BT}}. \tag{26}$$

Combining the latter two expressions and comparing to Planck's blackbody radiation formula

$$\rho(\omega) = \frac{\hbar}{\pi^2c^3}\frac{\omega^3}{e^{\frac{\hbar\omega}{k_BT}} - 1}, \tag{27}$$

we conclude that

$$B_{ab} = B_{ba},$$
$$B_{ba} = \frac{\pi^2c^3}{\omega^3\hbar}A_{ba},$$
$$A_{ba} = \frac{\omega^3}{3\pi c^3\epsilon_0\hbar}|\langle f|e\mathbf{r}|i\rangle|^2. \tag{28}$$

We have now obtained all three coefficients A_{ba}, B_{ba}, B_{ab} and the energy density $\rho(\omega)$ that appear in the rate Eqs. (22)–(23). Assuming initial conditions specified, e.g.,

$$N_b(t = 0) = N,$$
$$N_a(t = 0) = 0, \tag{29}$$

we can determine the level populations as a function of time. Note that Eqs. (22)–(23) reveal that indeed

$$N_a + N_b = N, \tag{30}$$

at all times. The only thing that remains in order to calculate level populations for a specific system is to determine the dipole matrix element (or momentum matrix element) in Eq. (28).

We shall next, in the spirit of the above model for transitions between levels associated with the same atom, generalize the concept by applying the Einstein rate equation model to examine electronic transition between different atoms *A* and *B*. In this way, we determine the occupation numbers of two levels on two dissimilar atoms (one level per atom) as a function of the distance between the two atoms. Instead of a transition rate (i.e., coefficients A_{ba}, B_{ba}, B_{ab}) governed by the dipole matrix element between two states on the same atom, the transition rate now depends on the dipole matrix element between an *A* atom state and a *B* atom state.

7. Overlap matrix elements

In this section, we calculate the overlap momentum integral between two *S* atomic levels associated with different atoms separated by a distance x_0. We choose a rectangular coordinate system oriented such that the line connecting the two atomic nuclei defines the x axis. The groundstate $(n, l, m) = (1, 0, 0)$ of the hydrogen-like atomic *S* state is

$$\psi_{100}(\mathbf{r}) = R_{10}(r)Y_{00}(\theta, \phi), \tag{31}$$

$$R_{10}(r) = 2\left(\frac{Z}{a_0}\right)^{3/2}\exp\left(-\frac{Zr}{a_0}\right), \tag{32}$$

$$Y_{00}\left(\theta, \phi\right) = \frac{1}{\sqrt{4\pi}}, \tag{33}$$

where Z is the atomic wave number and a_0 is the Bohr radius given by

$$a_0 = \frac{\hbar}{m_0c\alpha}. \tag{34}$$

Here, $\alpha \approx 1/137$ is the fine-structure constant. Normalization of wavefunctions requires

$$\langle\psi_{nlm}^i|\psi_{nlm}^i\rangle = 1, \tag{35}$$

where $i = 1$ ($i = 2$) for atom 1 (2). The overlap integral of groundstates associated with two atoms separated by a distance x_0 becomes

$$\begin{aligned}\langle\psi_{100}^2|\psi_{100}^1\rangle \;=\; & \frac{1}{\pi}\frac{1}{a_0^3}(Z_1Z_2)^{3/2} \\ & \times\int d^3\mathbf{r}\exp\left[-Z_1\sqrt{\left(\frac{x}{a_0}\right)^2 + \left(\frac{y}{a_0}\right)^2 + \left(\frac{z}{a_0}\right)^2}\right] \\ & \times\exp\left[-Z_2\sqrt{\left(\frac{x - x_0}{a_0}\right)^2 + \left(\frac{y}{a_0}\right)^2 + \left(\frac{z}{a_0}\right)^2}\right].\end{aligned} \tag{36}$$

In Fig. 4, we plot $\langle\psi_{100}^2|\psi_{100}^1\rangle$ as a function of the distance x_0 for the case where $Z_1 = Z_2 = 1$. Evidently, the overlap integral is equal to 1 when

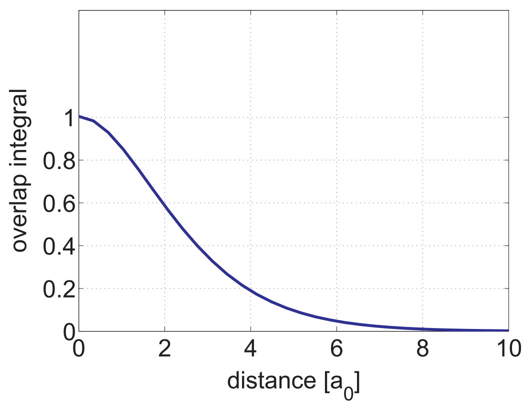

Fig. 4. Overlap integral $\langle \psi_{100}^2 | \psi_{100}^1 \rangle$ as a function of the distance x_0 between two atoms. Parameters are $Z_1 = Z_2 = 1$ and the distance is measured in units of the Bohr radius a_0. The calculation follows Eq. (36).

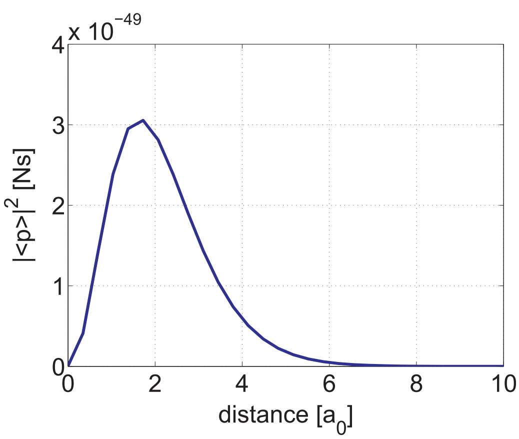

Fig. 5. Momentum overlap integral absolute squared, $|\langle \psi_{100}^2 | \mathbf{p} | \psi_{100}^1 \rangle|^2$, as a function of the distance x_0 between two atoms. Parameters are $Z_1 = Z_2 = 1$ and the distance is measured in units of the Bohr radius a_0. The calculation follows Eq. (37).

$x_0 = 0$ (as it must be when $Z_1 = Z_2 = 1$ to fulfill Eq. (35)). When the atoms separate more and more the overlap integral decreases fast and approaches zero.

We next compute the momentum matrix element $\langle \psi_{100}^2 | \mathbf{p} | \psi_{100}^1 \rangle$ that appears in the spontaneous emission rate given by Eq. (18). This is given by

$$\begin{aligned}\langle \psi_{100}^2 | \mathbf{p} | \psi_{100}^1 \rangle &= \frac{1}{\pi}\frac{i\hbar Z_1}{a_0^4}(Z_1 Z_2)^{3/2} \\ &\times \int d^3\mathbf{r}\, \exp\left[-Z_1\sqrt{\left(\frac{x}{a_0}\right)^2 + \left(\frac{y}{a_0}\right)^2 + \left(\frac{z}{a_0}\right)^2} \right] \\ &\left(\frac{\left(\frac{x}{a_0}\right)}{\sqrt{\left(\frac{x}{a_0}\right)^2 + \left(\frac{y}{a_0}\right)^2 + \left(\frac{z}{a_0}\right)^2}} \right) \\ &\times \exp\left[-Z_2\sqrt{\left(\frac{x-x_0}{a_0}\right)^2 + \left(\frac{y}{a_0}\right)^2 + \left(\frac{z}{a_0}\right)^2} \right].\end{aligned} \tag{37}$$

A comment is important here. The latter matrix element obviously does not necessarily display hermiticity, i.e., $\langle \psi_{100}^2 | \mathbf{p} | \psi_{100}^1 \rangle \neq \langle \psi_{100}^1 | \mathbf{p} | \psi_{100}^2 \rangle$ since Z_1 may not be equal to Z_2! We would not expect hermiticity, since atomic states calculated on separate atoms do not both fulfill the *same*

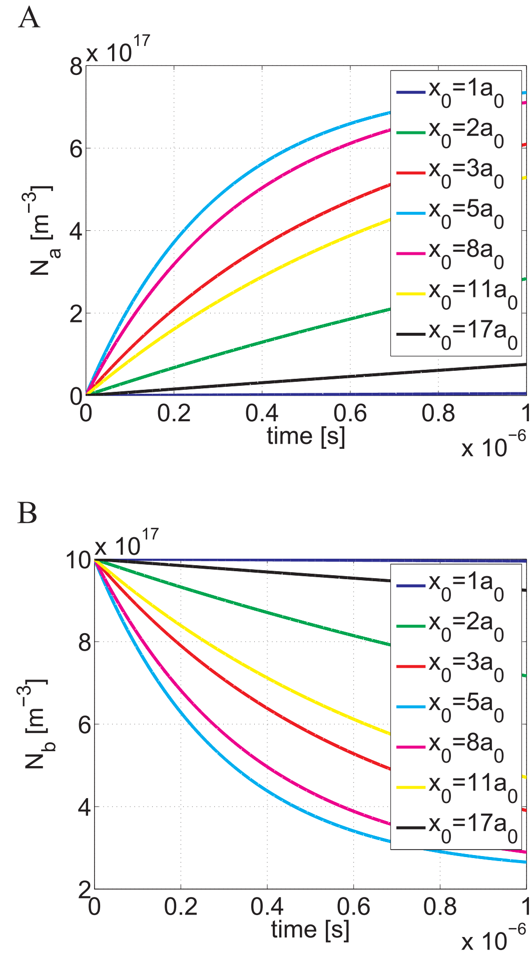

Fig. 6. Fixed distance in time between groups of atoms *A* and *B*. Temporal change in electron occupation of levels *A* and *B* as a function of time. Initially ($t = 0$), $N_b = N = 1 \cdot 10^{18}\ \mathrm{m}^{-3}$ and $N_a = 0$. Note that the net amount of emitted photons is equal to N_a at any time. The transition energy $\hbar\omega = E_B - E_A$ is set to 30 meV and the temperature is 300 K. The electron mass is set to the free-electron mass. Data are given for several fixed-in-time distances x_0 between groups *A* and *B*.

one-particle Hamiltonian (unless $Z_1 = Z_2$!). In principle, a two-particle Hamiltonian problem must be defined to restore hermiticity and this can easily be done. For our purposes, however, we are content with an approximate description of the momentum overlap between two distinct atoms.

In Fig. 5, we plot the absolute squared momentum overlap integral $|\langle \psi_{100}^2 | \mathbf{p} | \psi_{100}^1 \rangle|^2$ as a function of the distance x_0 in the case where $Z_1 = Z_2 = 1$. Evidently, the overlap integral equals 0 when $x_0 = 0$. This holds since $\mathbf{p}$ has parity -1 while ψ_{100}^1 and ψ_{100}^2 both have parity $+1$ under inversion. Note also that there is a maximum x_0^{max} of the momentum overlap integral at a distance between the two atomic nuclei around $1.5a_0$. When the atoms separate above x_0^{max}, the overlap integral decreases again and approaches zero at large separation distances. Hence, the groundstates of two atoms, both *S* parity, will generally couple optically (non-zero spontaneous emission rate) at all finite distances following the description in the previous sections. If one of the two states is a *P* state, the other a *S* state, the optical coupling is non-zero (and highest!) when $x_0 = 0$.

The above study reveals that electron transfer and light emission between dissimilar atoms depend heavily on the type of atoms involved, the symmetries of the interacting atomic levels, and the distance between the atoms.

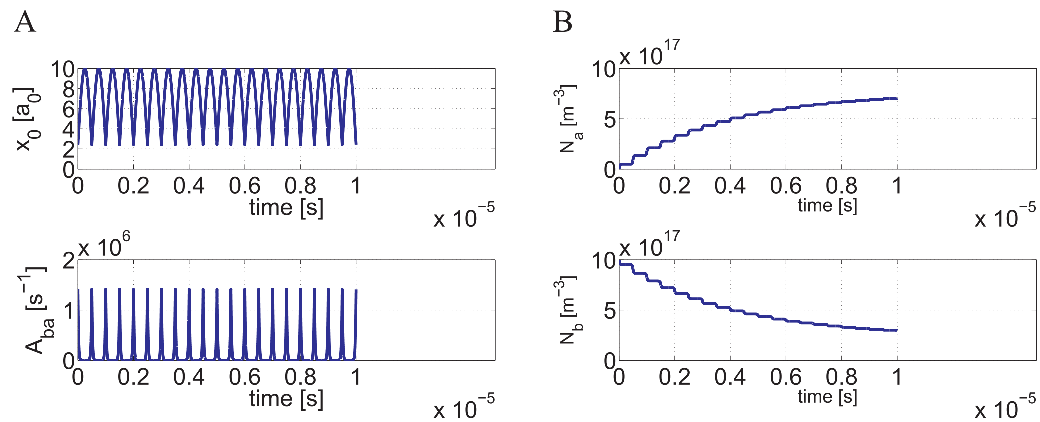

Fig. 7. Oscillatory distance in time between groups of atoms A and B. Temporal change in (left panel) distance x_0 and spontaneous emission rate A_{ba}, and (right panel) electron occupation of levels A and B as a function of time. Note that the net amount of emitted photons is equal to N_a at any time. Initially ($t = 0$), $N_b = N = 1{\cdot}10^{18}$ m^{-3} and $N_a = 0$. The transition energy $\hbar\omega = E_B - E_A$ is set to 30 meV and the temperature is 300 K. The electron mass is set to the free-electron mass.

7.1. Electron transfer and light emission in contact electrification - static operation

We have now made the preliminary analysis that allows us to compute quantitatively how contact electrification leads to transfer of electrons between systems of dissimilar atoms and light emission. To simplify matters, we shall assume that only transitions between the groundstates of atoms A and B take place, and that $E_B - E_A = \hbar\omega > 0$. We will examine this first for a number of atoms A interacting with a number of atoms B as a function of the average distance between the two systems of atoms. Initially, atoms B are assumed occupied while atoms A are vacant. The occupation numbers N_A and N_B of atoms A and B, respectively, are then studied as a function of time using the Einstein A and B rate equation model [Fig. 6]. The temporal relaxation rate of N_B depends strongly on the fixed-in-time distance x_0 between the two groups of atoms. Note that the net amount of emitted photons is equal to N_a at any time and $N_A + N_B = N$.

7.2. Electron transfer and light emission in contact electrification - dynamic operation

Next, we consider a typical dynamic triboelectric situation where a group of atoms A move periodically with respect to a group of atoms B. We compute the electron transfer and light emission as a function of time using the Einstein A and B rate equation model. Results are shown in Fig. 7 for the case where the distance x_0 between the two groups of atoms changes according to:

$$x_0[a_0] = 2.41 + (10 - 2.41)|\sin(2\pi{\cdot}10^6{\cdot}t[s])|, \quad (38)$$

corresponding to an oscillatory motion of period 1μ s in the distance between group A and B atoms. It's clear that the net transfer rate of electrons oscillates locally in time due to the oscillatory motion and deteriorates as N_b decreases with respect to N_a.

Finally, we point to that the above treatment of optical transitions between coupled atom systems can be generalized to larger interacting systems of atoms or solids using the density-matrix formalism to determine all level populations dynamically. This study will be pursued in a future work.

8. Conclusions

With the increasing importance of developing nano- and micro-scaled generators for powering networks of huge systems of sensors and the potential to harvest low-frequency ambient mechanical vibrations and ocean wave energy, much focus is given to understand the fundamental physical principles governing triboelectricity and triboelectric nanogenerator technology. We have presented a first quantum-mechanical model for electron transfer and light coupling between discrete levels in dissimilar and separated atoms. Our calculations show how the coupling changes with the (dynamic) separation of the atoms and reveal the importance of the wavefunction symmetries associated with the interacting atomic levels. The present model may set the scope for understanding electron transfer and photonic coupling in more complex systems such as two solids in contact and to exploit better the potential of triboelectric nanogenerators.

Acknowledgements

Morten Willatzen acknowledges financial support from a Talent 1000 Program for Foreign Experts, China.

References

[1] J. Henniker, Nature 196 (1962) 474.
[2] D. Davies, J. Phys. D: Appl. Phys. 2 (1969) 1533–1537.
[3] J. Lowell, J. Phys. D: Appl. Phys. 8 (1975) 53–63.
[4] W.R. Harper, Proc. R. Soc. A 205 (1951) 83–102.
[5] D.A. Hays, J. Chem. Phys. 61 (1974) 1455–1462.
[6] C. Liu, A.J. Bard, Chem. Phys. Lett. 480 (2009) 145–156.
[7] D.J. Lacks, R.M. Sankaran, J. Phys. D: Appl. Phys. 44 (2011) 453001.
[8] P. Shaw, Proc. R. Soc. Lond. Ser. A 94 (1917) 16–33.
[9] H.A. Mizes, E.M. Conwell, D.P. Salamida, Appl. Phys. Lett. 56 (1990) 1597–1599.
[10] J.A. Wiles, M. Fialkowski, M.R. Radowski, G.M. Whitesides, B.A. Grzybowski, J. Phys. Chem. B 108 (2004) 20296–20302.
[11] S. Wang, Y. Zi, Y.S. Zhou, S. Li, F. Fan, L. Lin, Z.L. Wang, J. Mater. Chem. A 4 (2016) 3728–3734.
[12] H. Baytekin, A. Patashinski, M. Branicki, B. Baytekin, S. Soh, B.A. Grzybowski, Science 333 (2011) 308–312.
[13] C. Xu, Y. Zi, A.C. Wang, H. Zou, X. He, P. Wang, Y.-C. Wang, P. Feng, D. Li, Z.L. Wang, Adv. Mater. (2018) 1706790.
[14] J. Chen, G. Zhu, W. Yang, Q. Jing, P. Bai, Y. Yang, T.-C. Hou, Z.L. Wang, Adv. Mater. 25 (2013) 6094–6099.
[15] J. Chen, Z.L. Wang, Joule 1 (2017) 480–521.
[16] Y. Zi, H. Guo, Z. Wen, M.-H. Yeh, C. Hu, Z.L. Wang, ACS Nano 10 (2016) 4797–4805.
[17] Z.L. Wang, L. Lin, J. Chen, S. Niu, Y. Zi, Triboelectric Nanogenerators, Green Energy and Technology, Springer, 2016.
[18] Z.L. Wang, Nat. Comment 542 (2017) 159–160.
[19] F.-R. Fan, Z.-Q. Tian, Z.L. Wang, Nano Energy 1 (2013) 328–334.
[20] Z.L. Wang, ACS Nano 7 (2013) 9533–9557.
[21] Z.L. Wang, J. Chen, L. Lin, Energy Environ. Sci. 8 (2015) 2250–2282.
[22] Z.L. Wang, G. Zhu, Y. Yang, S. Wang, C. Pan, Mater. Today 15 (2012) 532–543.
[23] Y. Yang, L. Lin, Y. Zhang, Q. Jing, T.-C. Hou, Z.L. Wang, ACS Nano 6 (2012) 10378–10383.
[24] G. Zhu, C. Pan, W. Guo, C.-Y. Chen, Y. Zhou, R. Yu, Z.L. Wang, Nano Lett. 12 (2012) 4960–4965.
[25] S. Wang, L. Lin, Y. Xie, Q. Jing, S. Niu, Z.L. Wang, Nano Lett. 13 (2013) 2282–2289.
[26] Y. Yang, Y.S. Zhou, H. Zhang, Y. Liu, S. Lee, Z.L. Wang, Adv. Mater. 25 (2013) 6594–6601.
[27] S. Wang, Y. Xie, S. Niu, L. Lin, Z.L. Wang, Adv. Mater. 26 (2014) 2818–2824.
[28] M. Willatzen, Theory of Gain in Bulk and Quantum-Well Semiconductor Lasers

(Ph.D. Thesis), Niels Bohr Institute, University of Copenhagen, 1993.
[29] D.J. Griffiths, Introduction to Quantum Mechanics, 2nd ed., PearsonPrentice Hall, Upper Saddle River, Jersey New, 2005, pp. 352–354.

Dr. Morten Willatzen is a Talent 1000 Foreign Expert and Senior Full Professor at the Beijing Institute of Nanoenergy and Nanosystems, Chinese Academy of Sciences. He also holds a Guest Professor position at the Department of Photonics Engineering, Technical University of Denmark and an Honorary Professorship at the Mads Clausen Institute, University of Southern Denmark. He received his MSc from Aarhus University and PhD from the Niels Bohr Institute at the University of Copenhagen. Morten Willatzen's research interests include solid state physics, mathematical physics, piezoelectricity, metamaterials and flow acoustics.

Dr. Zhong Lin Wang is a Hightower Chair and Regents's Professor at Georgia Tech. He is also the Chief scientist and Director for the Beijing Institute of Nanoenergy and Nanosystems, Chinese Academy of Sciences. His discovery and breakthroughs in developing nanogenerators establish the principle and technological road map for harvesting mechanical energy from environmental and biological systems for powering personal electronics. He coined and pioneered the field of piezotronics and piezo-phototronics by introducing piezoelectric potential gated charge transport process in fabricating new electronic and optoelectronic devices.